

# A Novel Concept for Balancing of the Phase Modules of a Three-Phase Unity Power Factor Y-Rectifier

Roland GREUL, Uwe DROFENIK, and Johann W. KOLAR

ETH Zurich, Power Electronic Systems Laboratory  
ETH-Zentrum / ETL H23, CH-8092 Zurich / SWITZERLAND  
Tel.: +41-1-632-2834 / Fax: +41-1-632-1212 / email: kolar@lem.ee.ethz.ch

**Abstract.** The isolated star point of a three-phase star-connection of single-phase unity power factor PWM rectifier systems (*Y-Rectifier*) results in a mutual coupling of the individual phase module outputs, i.e. the individual DC link voltage control loops. Starting from the theoretical analysis of a series connection of two DC/DC boost converters a control-oriented equivalent circuit of the three-phase *Y-Rectifier* system is derived in analytically closed form. Based on this a robust multi-variable control is designed which ensures constant DC link voltage levels for unsymmetric disturbances, i.e. step load changes of the phase modules. All theoretical findings are verified via numerical simulations.

## I. INTRODUCTION

For the realization of the input stage of high power telecommunications power supply systems a direct three-phase realization (Vienna Rectifier) or a star connection of three single-phase unity power factor PWM rectifier systems (*Y-Rectifier*, [1]) could be employed.

For the *Y-Rectifier* only a relatively low output voltage  $u_{O,i}$  of the phase modules is required for controlling the mains currents, [1], i.e.  $u_{O,i} = U_{O,i} = 400V$  has to be selected for operation in a wide input voltage range  $U_{N,i} = 320 \dots 530V_{rms}$  (line-to-line voltage). However, for the conversion of the phase module output voltages into the system output voltage  $U_{out} = 48V$  individual high-frequency isolated DC/DC converters have to be provided which are connected in parallel on the secondary side. The reference values of the DC/DC converter output currents are defined by the system output voltage control (cf. Fig.1 and Fig.2). Furthermore, the amplitudes of the *Y-Rectifier* mains phase currents are set by a feed-forward control such that the power supplied to a DC/DC converter ideally is balanced by the power drawn from the mains. Therefore, the DC link voltages  $u_{O,i}$  ideally should remain at a constant level. However, in practice a control of the DC link voltages has to be provided in order to account for non-idealities like losses of the DC/DC converter and rectifier stages.

Basically, the DC link voltage control can be performed oriented to the input, i.e. by increasing or decreasing the power drawn from the mains (cf. Fig.1(a)) or output-oriented, i.e. by changing the power supplied to the load (cf. Fig.1(b), [2]); the influence on the power supplied to the load then is compensated by the control of  $U_{out}$  (changing the power flow of all modules). In the literature this problem has not been paid much attention so far and only the concept depicted in Fig.1(b) has been described briefly [2] without detailed control-oriented analysis.

In this paper the control concept shown in Fig.1(a) is analyzed in detail. Due to the isolated star point  $N'$  of the modules each control action in a phase, i.e. the change of a module input voltage  $u_{U,i}$ , required for changing the module input current  $i_{N,i}$  takes influence also on the power consumption of the other modules. Accordingly, a mutual coupling of the phase modules is present which has to be considered for the design of the DC link voltage control. In Section II the overall system control structure is discussed and as a first step of deriving a control-oriented system model the mutual coupling of two series connected DC/DC boost converters with impressed individual output voltages is analyzed. There, for considering local average values of the system quantities over a

pulse period the module coupling can be formulated in analytically closed form what provides a direct insight into the physical system behavior. In a next step the small-signal converter model is extended to AC input resulting in a description of the two-phase operation of the *Y-Rectifier*. Finally, the three-phase system is analyzed and a model of the coupling of the phase modules is established. Based on this, a robust DC link voltage control is designed in Section III which ensures a constant level of the DC link voltages  $u_{O,i}$ . Topics to be treated in the continuation of the research are discussed in Section IV.

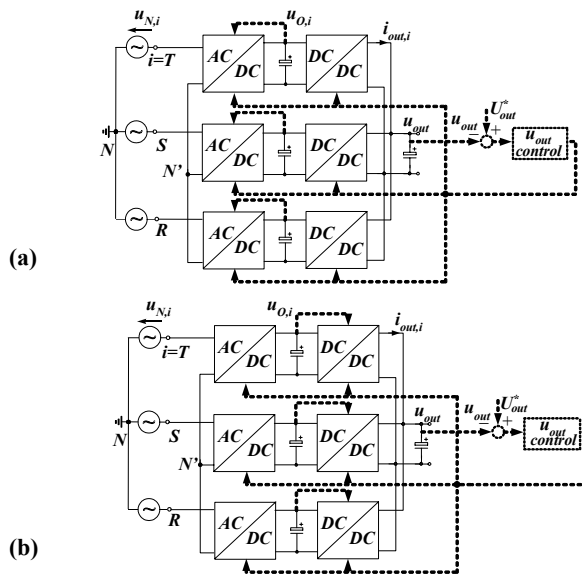


**Fig.1:** Control of the DC link voltages  $u_{O,i}$  of the phase modules of a *Y-Rectifier* [1] by changing the power drawn from the mains (input-oriented, cf. (a)) or by changing the power supplied to the load (output-oriented, cf. (b)).

## II. CONTROL ORIENTATED MODELING OF THE PHASE MODULE COUPLING

### 2.1 Control Structure of the Three-Phase System

The basic structure of the *Y-Rectifier* power circuit and of a control concept which allows a continuation of the system operation also in case of a mains phase loss or for heavily unbalanced mains is shown in Fig.2. There, the control of the phase module DC link voltages  $u_{O,i}$  is implemented according to Fig.1(a).

In order to reduce the converter conduction losses two simultaneously controlled power transistors  $S_{i,1}$  and  $S_{i,2}$ ,  $i=1,2,3$ , are employed in each module. This avoids the output diode conduction losses of a conventional boost-type unity power factor rectifier and reduces the diode bridge input losses as the current of one conducting diode is always shared with the power transistor connected in parallel. For  $U_{O,i} = 400V$  ultra-fast recovery diodes  $D_{N,i}$  with  $600V$  blocking capability can be employed what results in low power transistor turn-on losses. Therefore, a high efficiency of the energy conversion can be achieved also for high switching frequency.

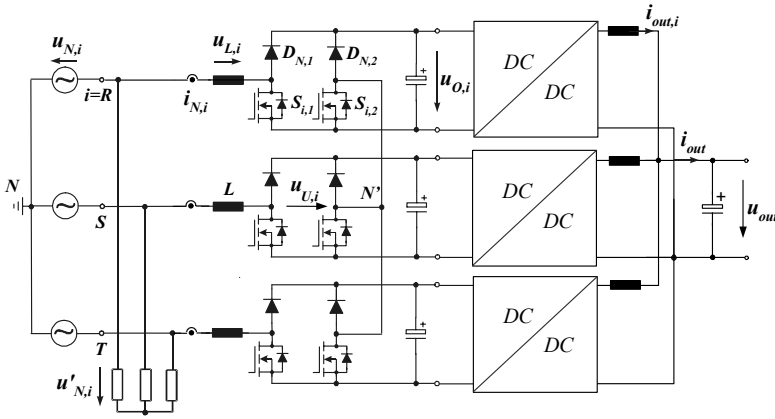
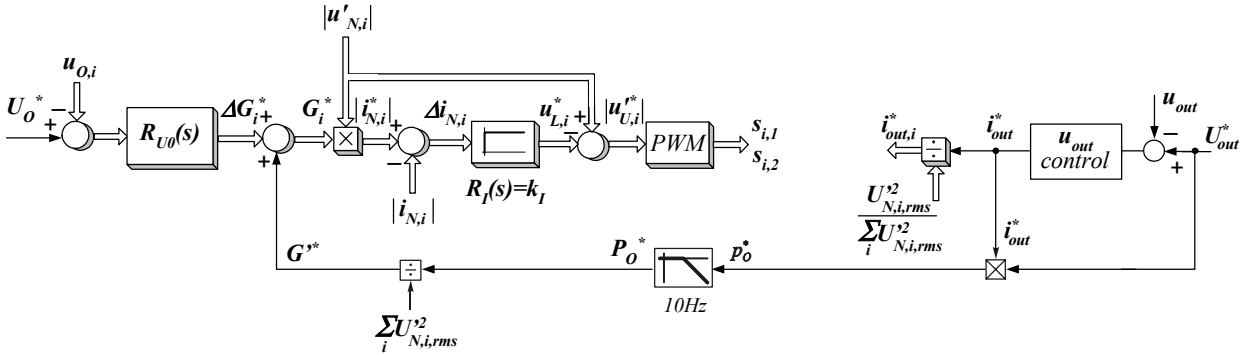


**Fig.2:** Structure of the power circuit and of the control of a two-level *Y-Rectifier* [1]. Signal paths being equal for all phases are combined in double lines. The zero-sequence free components  $u_{N,i}'$  of the actual mains phase voltages  $u_{N,i}$  are derived by a star-connection of equal ohmic resistors. For determining the phase module input voltage reference values  $u_{U,i}'$  the reference values  $u_{L,i}^*$  of the voltages across an input inductor  $L$  which are defined by the phase current controls are extended by mains voltage feedforward signal  $u_{N,i}'$ . There, for full utilization of the modulation range a third harmonic has to be considered which can be derived with low effort from a three-phase rectification of the measured values of the phase voltages  $u_{N,i}'$  [3].



The reference value  $i_{out}^*$  of the system total output current is set by the output voltage control. The distribution of  $i_{out}^*$  to the individual DC/DC converters is under consideration of the mains phase voltage condition such that the resulting fundamental mains behavior of the three-phase system is equivalent to a symmetric three-phase ohmic load. Accordingly, for defining the mains phase current reference values  $i_{N,i}^*$  which are set by an underlying current control a reference conductance  $G^*$  which is equivalent to  $i_{out}^*$  concerning the power flow is multiplied with the measured zero-sequence free components  $u_{N,i}'$  of the mains phase voltages.

For ensuring a constant DC link voltage  $u_{O,i} = U_{O,i}$  the DC link voltage control (cf. controller  $R_{U0}(s)$  in Fig.2) changes the reference conductance  $G^*$  defined by the input power feedforward equally for all modules by  $\Delta G_i^*$  what results in an increase or decrease of the corresponding phase current amplitude and/or of the power fed into the DC link. As the isolated star point  $N'$  is forcing the sum of the phase currents  $i_{N,i}$  to zero, there each control action takes influence on all phase modules, i.e. a mutual coupling of the DC link voltage control loops is present. Therefore, the control design has to be performed for a multi-variable system where a decoupling of the phase controls should be achieved.

## 2.2 Series Connection of DC/DC Boost Converters

In order to gain insight into the coupling of the phase modules of the three-phase system in a first step a series connection of two DC/DC boost converters *a, b* (cf. Fig.3(a)) with impressed constant output voltages  $U_{O,a}$  and  $U_{O,b}$  is analyzed. There, both converters are assumed to operate in the continuous conduction mode.

In Fig.4 the control-oriented block diagram of the system based on local average values of the quantities within a pulse period is depicted in combination with an individual current control for each converter. In analogy to the three-phase system the input current reference value is determined by multiplying the equally split input voltage and the reference conductance.

A change of the input conductance reference value of system *a* by  $\Delta G_a^*$  ( $\Delta G_b^* = 0$ ) and/or of the input current reference value by  $\Delta I_a^*$  results in a change  $\Delta I_{D,a}$  of the average value of the related output diode current  $i_{D,a}$ . In order to set a positive change  $\Delta I_a^*$  the relative turn-on time  $d_a$  of power transistor  $S_a$  is increased by the current controller  $R_{I,a}(s)$ . The current controller  $R_{I,b}(s)$  ( $R_{I,a}(s) = R_{I,b}(s) = k_I$ ) now tries to compensate the resulting change of the input current (which is common to both systems) by increasing the relative turn-off time  $d_b' = (1 - d_b)$  of  $S_b$ .

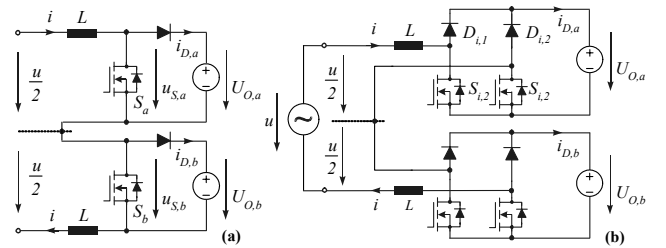


**Fig.3:** (a) Series connection of two DC/DC boost converters and (b) series connection of two single-phase boost-type unity power factor rectifier systems being equivalent to two-phase operation of the *Y-Rectifier* occurring for a mains phase loss. The output voltages  $U_{O,a}$  and  $U_{O,b}$  are assumed constant.

As the output diode current is determined by the product of the input current and the transistor turn-off time, finally an increase or a decrease  $\Delta I_{D,a}$  of  $I_{D,a}$  will occur dependent on the final increase of the input current  $I = I_a = I_b$  and decrease of  $d_a$ . However, in any case the output diode current  $I_{D,b}$  of system *b* will be increased by  $\Delta I_{D,b}$ . This consideration is discussed in detail in the following.

In the following, the system transfer behavior and the coupling of the individual systems *a* and *b* is described for the DC/DC and AC/DC case by coefficients

$$H_{ii,\omega=0} = \frac{\Delta I_{D,i}}{\Delta I_i^*} \quad H_{ij,\omega=0} = \frac{\Delta I_{D,j}}{\Delta I_i^*} \quad (1)$$

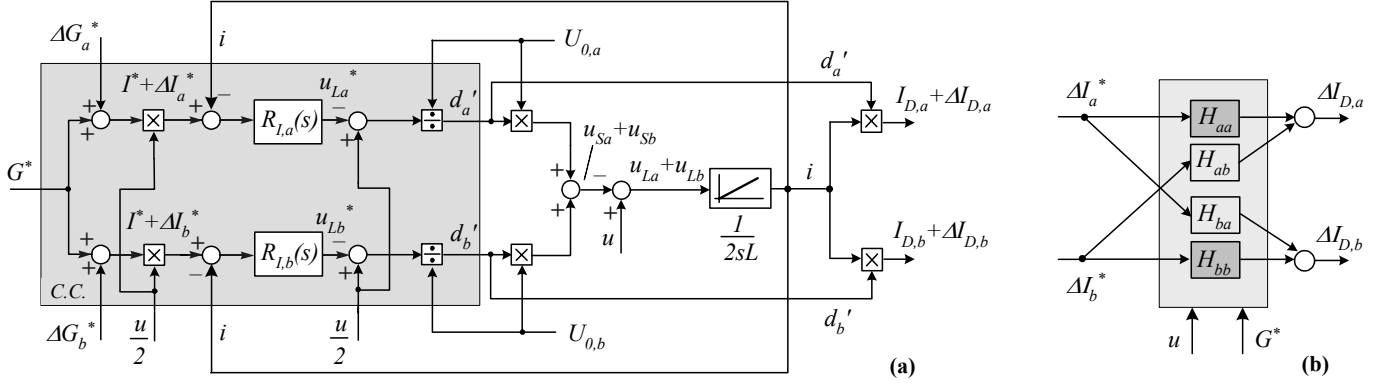


**Fig.4:** (a) Control-oriented block diagram of the input current control and of the power circuit of the system according to Fig.3(a) and (b) representation as multi-variable control system characterized by stationary coupling coefficients  $H_{ii}$  and  $H_{ji}$ ,  $i,a,b$  (cf. (1)).

where  $i,j = a,b$ . As the crossover frequency of the DC link voltage control loops is significantly lower than the mains frequency (typ. at 5...10Hz) only the transfer behavior at low frequencies is of interest. Therefore, for limiting to the essentials only the DC values  $H_{ii,\omega=0}$  and  $H_{ij,\omega=0}$  are considered and the output voltages  $U_{0,a}$ ,  $U_{0,b}$  are assumed constant. As a more detailed analysis shows,  $H_{ii,\omega=0}$  and  $H_{ij,\omega=0}$  represent a good approximation of the low frequency behavior of the actual transfer functions  $H_{ii}(s)$  and  $H_{ij}(s)$  for frequencies lower than 10Hz for practical systems and are therefore sufficient for controller design. For the sake of brevity the index  $\omega=0$  is omitted in the following. For an analytical calculation of the coupling coefficients we define

$$\tilde{I}_a = \tilde{I}_b = \tilde{I} = I + \Delta I \quad (2)$$

as the phase current of each partial system in Fig.3(a) and/or Fig.4 including a small-signal deviation caused by  $\Delta I_a^*$  or  $\Delta I_b^*$ . Assuming an approximately ideal setting of the current reference values  $I_a^* = I_b^*$ ,

$$I_a^* = I_b^* = I \quad (3)$$

the reference currents can be given as

$$\begin{aligned} \tilde{I}_a^* &= I_a^* + \Delta I_a^* = I + \Delta I_a^* \\ \tilde{I}_b^* &= I_b^* + \Delta I_b^* = I + \Delta I_b^* \end{aligned} \quad (4)$$

The output diode currents including small-signal deviations

$$\begin{aligned} \tilde{I}_{D,a} &= I_{D,a} + \Delta I_{D,a} \\ \tilde{I}_{D,b} &= I_{D,b} + \Delta I_{D,b} \end{aligned} \quad (5)$$

are dependent on the boost converter duty cycles,

$$\begin{aligned} I_{D,a} &= D_a' I_a \\ I_{D,b} &= D_b' I_b \end{aligned} \quad (6)$$

or

$$\begin{aligned} \tilde{I}_{D,a} &= D_a' \tilde{I}_a \\ \tilde{I}_{D,b} &= D_b' \tilde{I}_b \end{aligned} \quad (7)$$

Assuming constant output voltages

$$U_{0,a} = U_{0,b} = U_0 \quad (8)$$

and operation in continuous conduction mode, the local average value of the switch voltage is

$$\begin{aligned} U_{S,a} &= D_a' U_0 \\ U_{S,b} &= D_b' U_0 \end{aligned} \quad (9)$$

Considering (2), (3) and (4) the off-time  $D_i' = 1 - D_i$  of the switches can now be written as (cf. Fig.4)

$$\begin{aligned} D_a' &= \frac{1}{U_0} \left[ \frac{1}{2} U - k_I (\tilde{I}_a^* - \tilde{I}_a) \right] = \frac{1}{U_0} \left[ \frac{1}{2} U - k_I (\Delta I_a^* - \Delta I) \right] \\ D_b' &= \frac{1}{U_0} \left[ \frac{1}{2} U - k_I (\tilde{I}_b^* - \tilde{I}_b) \right] = \frac{1}{U_0} \left[ \frac{1}{2} U - k_I (\Delta I_b^* - \Delta I) \right] \end{aligned} \quad (10)$$

As our considerations are referring to stationary operation ( $d/dt \rightarrow 0$ ) we have for the relation of the input voltage and the voltage across the switches (cf. Fig.3(a))

$$U = U_{S,a} + U_{S,b} = U_0 (D_a' + D_b') \quad (11)$$

Substituting the relative off-times in (10) by (11) results in

$$\begin{aligned} \frac{1}{U_0} U &= D_a' + D_b' = \frac{1}{U_0} U - \frac{1}{U_0} k_I (\Delta I_a^* + \Delta I_b^* - 2\Delta I) \\ \rightarrow \Delta I &= \frac{1}{2} \Delta I_a^* + \frac{1}{2} \Delta I_b^* \end{aligned} \quad (12)$$

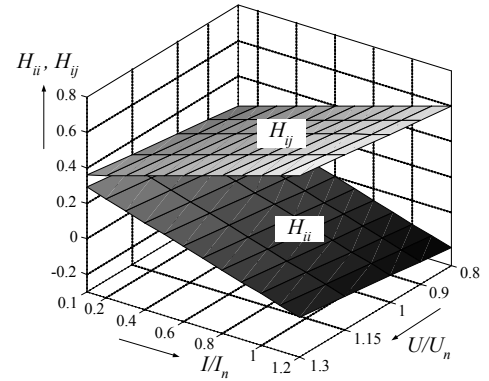


**Fig.5:** Stationary coupling coefficients  $H_{ii}$  and  $H_{ij}$  according to Fig.4(b) and/or (16) in dependency of the normalized input voltage amplitude and the normalized phase current. Due to the symmetry of the system (cf. Fig.3(a))  $H_{aa} = H_{bb}$  and  $H_{ba} = H_{ab}$  is valid. The normalization basis is  $U_n = 400V$  and  $I_n = 2P_n/U_n = 17.5A$  ( $P_n = 3500W$  per module). The assumed gain  $k_I = 15.2VA^{-1}$  of the P-type current control is identical to the controller gain given for the high quality current control of a phase module with sinusoidal input voltage  $U_{N,I} = 320 \dots 520V_{rms}$ , output voltage  $U_0 = 400V$ , and an output power range of  $P_{out} = 560W \dots 10.1kW$ .

Employing (7) and (10) gives

$$\begin{aligned} \tilde{I}_{D,a} &= D_a' \tilde{I}_a = \frac{1}{U_0} \left[ \frac{1}{2} U \tilde{I}_a - k_I \tilde{I}_a (\tilde{I}_a^* - \tilde{I}_a) \right] \\ \tilde{I}_{D,b} &= D_b' \tilde{I}_b = \frac{1}{U_0} \left[ \frac{1}{2} U \tilde{I}_b - k_I \tilde{I}_b (\tilde{I}_b^* - \tilde{I}_b) \right] \end{aligned} \quad (13)$$

and we receive for the small-signal deviations by using (4), (5) and (12)

$$\begin{aligned} \Delta I_{D,a} &= \frac{1}{2U_0} (\frac{1}{2} U - k_I I) \Delta I_a^* + \frac{1}{2U_0} (\frac{1}{2} U + k_I I) \Delta I_b^* \\ \Delta I_{D,b} &= \frac{1}{2U_0} (\frac{1}{2} U + k_I I) \Delta I_a^* + \frac{1}{2U_0} (\frac{1}{2} U - k_I I) \Delta I_b^* \end{aligned} \quad (14)$$

which can also be written as

$$\begin{pmatrix} \Delta I_{D,a} \\ \Delta I_{D,b} \end{pmatrix} = \underline{H} \cdot \begin{pmatrix} \Delta I_a^* \\ \Delta I_b^* \end{pmatrix} = \begin{pmatrix} H_{aa} & H_{ab} \\ H_{ba} & H_{bb} \end{pmatrix} \cdot \begin{pmatrix} \Delta I_a^* \\ \Delta I_b^* \end{pmatrix} \quad (15)$$

with the matrix elements defined in (1)

$$\begin{aligned} H_{ii} &= \frac{1/2}{U_0} (\frac{1}{2}U - k_I I) \\ H_{ij} &= \frac{1/2}{U_0} (\frac{1}{2}U + k_I I) \end{aligned} \quad (16)$$

In correspondence to the foregoing discussion a positive cross coupling  $H_{ij}$  is present independent of the operating condition. The direct coupling  $H_{ii}$  shows a comparably low absolute value and exhibits a negative sign for high power and low input voltage, cf. (16) and/or **Fig.5**. According to Fig.5 for controlling  $U_{O,a}$  and/or  $U_{O,b}$  via  $\Delta I_a^*$  and/or  $\Delta I_b^*$  a decoupling has to be provided. Alternatively, the weak direct coupling could be neglected in a first approximation and the DC link voltage control could only rely on the pronounced cross coupling, i.e.  $U_{O,a}$  could be controlled by  $\Delta I_b^*$  and  $\Delta I_a^*$  could be employed for controlling  $U_{O,b}$ .

**Remark:** A reference current deviation  $\Delta I_a^* \neq \Delta I_b^*$  (cf. (15)) cannot be fully set by the current control but provides means to take influence on the relative turn-off time of the switches and, therefore on the average current fed into the partial output voltages  $U_{O,a}$  and  $U_{O,b}$ . Only for  $\Delta I_a^* = \Delta I_b^* = \Delta I$  the control can adjust the actual current accordingly what results according to (15) and (16) in  $\Delta I_{D,a} = \Delta I_{D,b} = \Delta I_D = U/(2U_0) \cdot \Delta I$ . Considering the power balance between input and output side and the relationship between voltage transfer ratio and relative switch turn-off time,  $D' = (U/2)/U_0$ , we receive exactly the same result. This gives a clear indication of the correctness of the derived system model.

### 2.3 Series Connection of Single-Phase AC/DC Boost Converters

For replacing the DC input voltage in Fig.3(a) by an AC voltage (cf. Fig.3(b)) the behavior of the *Y-Rectifier* for two-phase operation, i.e. in case of a mains phase loss can be determined. Deviating the reference conductance by  $\Delta G_i^*$  now results in a change  $\Delta \hat{I}_i^*$  of the amplitude  $\hat{I}_i^*$  of the related phase current reference value  $i_i^*$ . Due to the low dynamics of the output voltage control only the change  $\Delta I_{D,a}$  and  $\Delta I_{D,b}$  of the diode current average values has to be considered. Accordingly, the sinusoidal shape of the input voltage and current does not take direct influence and the system control behavior can be characterized by coupling coefficients

$$H_{ii} = \frac{\Delta I_{D,i}}{\Delta \hat{I}_i^*} \quad H_{ij} = \frac{\Delta I_{D,j}}{\Delta \hat{I}_i^*} \quad (17)$$

( $i,j=a,b$ ) For an analytical calculation of  $H_{ii}$  and  $H_{ij}$  we assume a purely sinusoidal AC input voltage

$$u = \hat{U} \cos \omega t = \sqrt{2} U_{rms} \cos \omega t \quad (18)$$

and a rectified phase current at the DC-side

$$i = \hat{I} |\cos \omega t| = \sqrt{2} I_{rms} |\cos \omega t| \rightarrow i > 0 \quad (19)$$

In analogy to section 2.2 the actual phase current is now defined under consideration of a small-signal deviation amplitude as

$$\tilde{i}_a = \tilde{i}_b = \tilde{i} = (\hat{I} + \Delta \hat{I}) |\cos \omega t|, \quad (20)$$

where the reference currents are given as

$$\begin{aligned} \tilde{i}_a^* &= (\hat{I}_a^* + \Delta \hat{I}_a^*) |\cos \omega t| = (\hat{I} + \Delta \hat{I}_a^*) |\cos \omega t|, \\ \tilde{i}_b^* &= (\hat{I}_b^* + \Delta \hat{I}_b^*) |\cos \omega t| = (\hat{I} + \Delta \hat{I}_b^*) |\cos \omega t| \end{aligned} \quad (21)$$

and the diode currents can be written in general form as

$$\begin{aligned} \tilde{i}_{D,a} &= i_{D,a} + \Delta i_{D,a} = d_a' \tilde{i}_a^* \\ \tilde{i}_{D,b} &= i_{D,b} + \Delta i_{D,b} = d_b' \tilde{i}_b^* \end{aligned} \quad (22)$$

Proceeding further in analogy to the previous section we finally receive

$$\begin{aligned} \begin{pmatrix} \Delta i_{D,a} \\ \Delta i_{D,b} \end{pmatrix}_{AC} &= \begin{pmatrix} h_{aa}(\omega t) & h_{ab}(\omega t) \\ h_{ba}(\omega t) & h_{bb}(\omega t) \end{pmatrix} \cdot \begin{pmatrix} \Delta \hat{I}_a^* \\ \Delta \hat{I}_b^* \end{pmatrix} = \\ &= \frac{\cos^2 \omega t}{2U_0} \begin{pmatrix} \frac{1}{2}\hat{U} - k_I \hat{I} & \frac{1}{2}\hat{U} + k_I \hat{I} \\ \frac{1}{2}\hat{U} + k_I \hat{I} & \frac{1}{2}\hat{U} - k_I \hat{I} \end{pmatrix} \cdot \begin{pmatrix} \Delta \hat{I}_a^* \\ \Delta \hat{I}_b^* \end{pmatrix} \end{aligned} \quad (23)$$

The average value of the time-dependent coefficients  $h_{ii}(\omega t)$  and  $h_{ij}(\omega t)$  now is found via integration over one mains period as

$$\begin{aligned} H_{ii,AC} &= \frac{1}{2\pi} \int_0^{2\pi} h_{ii,AC}(\omega t) d(\omega t) = \frac{1/4}{U_0} (\frac{1}{2}\hat{U} - k_I \hat{I}) \\ H_{ij,AC} &= \frac{1}{2\pi} \int_0^{2\pi} h_{ij,AC}(\omega t) d(\omega t) = \frac{1/4}{U_0} (\frac{1}{2}\hat{U} + k_I \hat{I}) \end{aligned} \quad (24)$$

with

$$\begin{aligned} \begin{pmatrix} \Delta I_{D,a} \\ \Delta I_{D,b} \end{pmatrix}_{AC} &= \underline{H} \cdot \begin{pmatrix} \Delta \hat{I}_a^* \\ \Delta \hat{I}_b^* \end{pmatrix} = \\ &= \frac{1}{4U_0} \begin{pmatrix} \frac{1}{2}\hat{U} - k_I \hat{I} & \frac{1}{2}\hat{U} + k_I \hat{I} \\ \frac{1}{2}\hat{U} + k_I \hat{I} & \frac{1}{2}\hat{U} - k_I \hat{I} \end{pmatrix} \cdot \begin{pmatrix} \Delta \hat{I}_a^* \\ \Delta \hat{I}_b^* \end{pmatrix} \end{aligned} \quad (25)$$

describing the coupling characteristic according to (17).

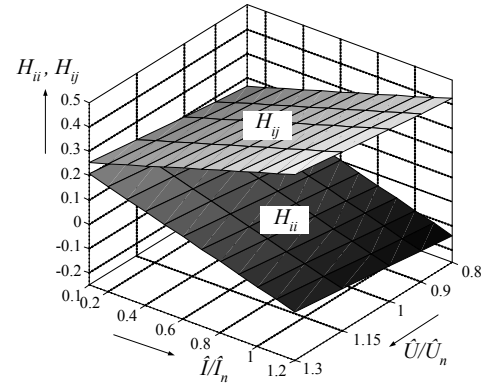


**Fig.6:** Stationary changes  $\Delta I_{D,i}$ ,  $\Delta I_{D,j}$  of the output diode average current values of the system shown in Fig.4(b) as resulting from a stationary small signal change  $\Delta \hat{I}_i^*$  of the amplitude  $\hat{I}_i^*$  of the input current reference value  $i_i^*$  of phase  $i$ . Representation (in dependency on normalized input voltage amplitude  $\hat{U}_n=400\sqrt{2}=563V$  and normalized phase current  $\hat{I}_n=4P_n/\hat{U}_n=24.9A$  with  $P_n=3500W$  for each rectifier module) based on the coupling coefficients  $H_{ii}=\Delta I_{D,i}/\Delta \hat{I}_i^*$  and  $H_{ij}=\Delta I_{D,j}/\Delta \hat{I}_i^*$  (as defined in (17)). Due to the system symmetry  $H_{aa}=H_{bb}$  and  $H_{ab}=H_{ba}$  is valid. Simulation parameters and current gain  $k_I$  as for Fig.5.

Comparing the coupling coefficients of the single phase AC/DC system (24) to the coefficients of the DC/DC system (16) for equal output power we have the relation

$$\underline{H}_{AC/DC} = \frac{1}{\sqrt{2}} \underline{H}_{DC/DC} \quad (26)$$

(cf. Fig.5 and Fig.6) which also directly follows from relating the DC values to the rms values of the AC quantities, i.e.  $U_{DC}=1/\sqrt{2} \cdot \hat{U}$

and  $I_{DC}=1/\sqrt{2}\hat{I}$  and clearly proof the physical correctness of the considerations.

Based on (25) a decoupling of the control of  $U_{O,a}$  and  $U_{O,b}$  could be performed, where we have for the decoupling matrix, i.e. for the inverse of the system matrix

$$\underline{M}_{DEC} = \underline{H}^{-1} = \frac{U_0}{\frac{1}{2}\hat{U}k_I\hat{I}} \begin{pmatrix} k_I\hat{I} - \frac{1}{2}\hat{U} & k_I\hat{I} + \frac{1}{2}\hat{U} \\ k_I\hat{I} + \frac{1}{2}\hat{U} & k_I\hat{I} - \frac{1}{2}\hat{U} \end{pmatrix}. \quad (27)$$

## 2.4 Y-Rectifier Operating at Symmetric Three-Phase Mains

After having gained insight into the system characteristic for two-phase operation now the behavior for three-phase input voltage should be analyzed. For changing the reference input conductance  $\Delta G_i^*$ ,  $i=R,S,T$ , of a phase module and/or the phase module input current reference value amplitude  $\Delta \hat{I}_i^*$  a related change  $\Delta I_{D,i}$  of the output diode current average values of *all* modules will occur. This is due the mutual coupling of the phases caused by the isolated module star point  $N'$  where trying to introduce a deviation from the  $i_R+i_S+i_T=0$  according to  $\Delta \hat{I}_i^*$  for the module in phase  $i$  takes influence on the currents and the relative switch turn-off times (i.e. the diode output current) of all other phases.

A control-oriented block diagram of the system is depicted in **Fig.7**. The stationary coupling coefficients which have to be considered for the design of the control of the DC link voltages  $U_{O,i}$  are derived in the following.

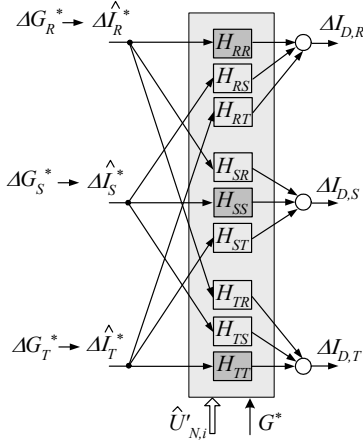


**Fig.7:** Block diagram representation of the three-phase Y-Rectifier showing the stationary influence of changes  $\Delta \hat{I}_i^*$  of the amplitudes  $\hat{I}_i^*$  of the input current reference values  $i_i^*$  on the phase module output diode current average values.

For a general analytical calculation of the coupling coefficients of the three-phase AC/DC converter we define AC-side phase voltages

$$\begin{aligned} u_R &= \hat{U}_R \cos(\omega t - \varphi_R) = \hat{U}_R \cos \omega t \\ u_S &= \hat{U}_S \cos(\omega t - \varphi_S) = \hat{U}_S \cos(\omega t - \frac{2\pi}{3}) \\ u_T &= \hat{U}_T \cos(\omega t - \varphi_T) = \hat{U}_T \cos(\omega t - \frac{4\pi}{3}) \end{aligned} \quad (28)$$

with  $\varphi_R=0$ ,  $\varphi_S=2\pi/3$ ,  $\varphi_T=4\pi/3$  and rectified DC-side phase currents

$$\begin{aligned} i_R &= \hat{I}_R \left| \cos \omega t \right| \\ i_S &= \hat{I}_S \left| \cos(\omega t - \frac{2\pi}{3}) \right| \\ i_T &= \hat{I}_T \left| \cos(\omega t - \frac{4\pi}{3}) \right| \end{aligned} \quad \rightarrow i_{R,S,T} > 0 \quad (29)$$

The sum of the AC-side phase currents has to be zero which is described by the condition

$$\text{sgn}(i_R) i_R + \text{sgn}(i_S) i_S + \text{sgn}(i_T) i_T = 0. \quad (30)$$

Defining small-signal deviations in analogy to Section 2.2 and/or Section 2.3, and assuming in a first step an ideal control of the not deviated phase current reference values, a constant output voltage

of the modules and restricting the consideration to the quasi-stationary behavior ( $d/dt \rightarrow 0$ ) we receive employing (28) – (30),

$$\begin{pmatrix} \Delta i_{D,R} \\ \Delta i_{D,S} \\ \Delta i_{D,T} \end{pmatrix} = \begin{pmatrix} h_{RR}(\omega t) & h_{RS}(\omega t) & h_{RT}(\omega t) \\ h_{SR}(\omega t) & h_{SS}(\omega t) & h_{ST}(\omega t) \\ h_{TR}(\omega t) & h_{TS}(\omega t) & h_{TT}(\omega t) \end{pmatrix} \cdot \begin{pmatrix} \Delta \hat{I}_R^* \\ \Delta \hat{I}_S^* \\ \Delta \hat{I}_T^* \end{pmatrix} \quad (31)$$

with time-dependent coefficients

$$\begin{aligned} h_{ii}(\omega t) &= +\frac{1}{3U_0} (2\hat{U}_i - k_I \hat{I}_i) \cos^2(\omega t - \varphi_i) \\ h_{ij}(\omega t) &= -\frac{1}{3U_0} (\hat{U}_i + k_I \hat{I}_i) \cos(\omega t - \varphi_i) \cos(\omega t - \varphi_j) \end{aligned} \quad (32)$$

The coupling coefficients characterizing the Y-Rectifier then result from integration over a mains period as

$$\begin{aligned} H_{ii} &= \frac{1}{2\pi} \int_0^{2\pi} h_{ii}(\omega t) d(\omega t) = \frac{1}{3U_0} (\hat{U}_i - \frac{1}{2} k_I \hat{I}_i) \\ H_{ij} &= \frac{1}{2\pi} \int_0^{2\pi} h_{ij}(\omega t) d(\omega t) = \frac{1}{12U_0} (\hat{U}_i + k_I \hat{I}_i) \end{aligned} \quad (33)$$

Summarizing the system behavior in matrix form we have

$$\begin{pmatrix} \Delta I_{D,R} \\ \Delta I_{D,S} \\ \Delta I_{D,T} \end{pmatrix} = \underline{H} \cdot \begin{pmatrix} \Delta \hat{I}_R^* \\ \Delta \hat{I}_S^* \\ \Delta \hat{I}_T^* \end{pmatrix} = \begin{pmatrix} H_{RR} & H_{RS} & H_{RT} \\ H_{SR} & H_{SS} & H_{ST} \\ H_{TR} & H_{TS} & H_{TT} \end{pmatrix} \cdot \begin{pmatrix} \Delta \hat{I}_R^* \\ \Delta \hat{I}_S^* \\ \Delta \hat{I}_T^* \end{pmatrix} \quad (34)$$

with  $i, j = R, S, T$ .

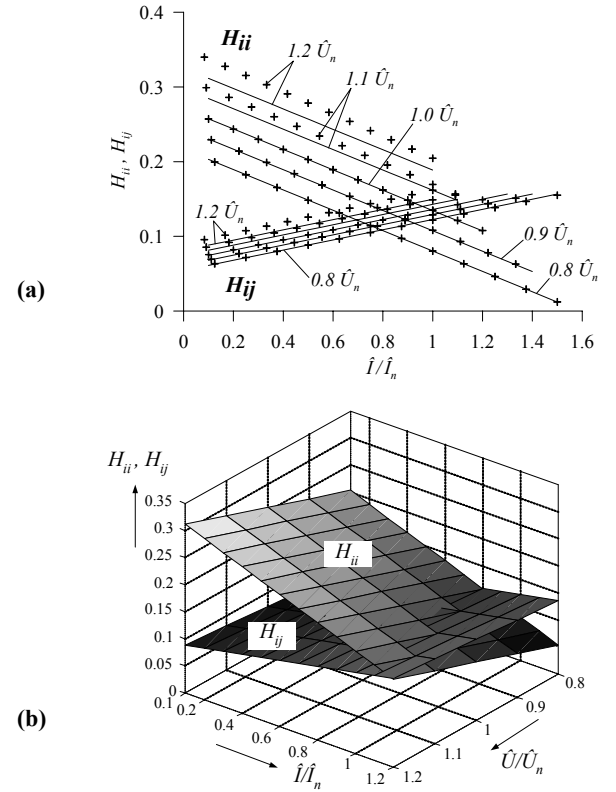


**Fig.8:** (a) Comparison of the stationary coupling coefficients  $H_{ii}$  and  $H_{ij}$  of the Y-Rectifier as resulting from digital simulation (data points marked by “+”) and analytical calculation (cf. (33), solid lines). (b) Three-dimensional representation of (a). Current gain  $k_I=15.2$ ; system parameters as for Fig.5; normalization basis  $\hat{U}_{N,n}=325V$ ,  $\hat{I}_n=P_n/(\hat{U}_{N,n}/2)$  ( $P_n=3500W$  for each module, i.e. 10kW total system output power).

A comparison of the analytically calculated stationary coupling coefficients  $H_{ii}$  and  $H_{ij}$  and results of digital simulations is given in **Fig.8(a)** for a current controller gain of  $k_I=15.2$  and clearly underlines the high accuracy of the modelling approach.

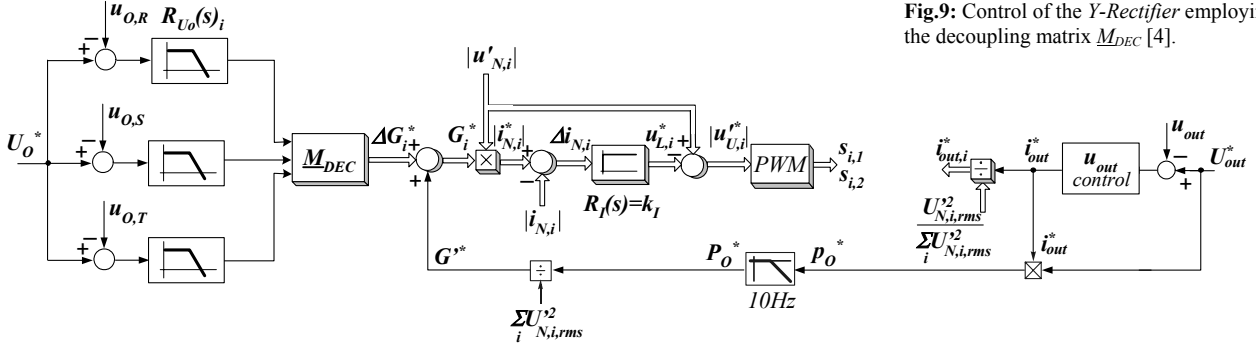


**Fig.9:** Control of the *Y-Rectifier* employing the decoupling matrix  $\underline{M}_{DEC}$  [4].

**Remark:** One has to point out that for deriving the system model the small-signal phase current deviations are assumed to show a sinusoidal shape *in phase* with the according phase current (cf. (20)). As compared to considering the phase displacement  $\varphi_{ii^*}$  of the actual and reference current occurring in practice, this considerably simplifies the calculations and can be justified by the fact that the influence on the transferred power is only by  $\cos\varphi_{ii^*}$  which shows values close to 1 for low values of  $\varphi_{ii^*}$ . The resulting analytical expressions are then of low complexity and provide useful guidelines (cf. (36)) for designing a stable system control and/or for decoupling the DC link voltage control loops of the phase modules.

### III. DESIGNING A DC-LINK VOLTAGE CONTROL FOR SYMMETRIC MAINS

For ideal decoupling, we would have for the resulting matrix elements  $H_{ii}=1$  and  $H_{ij}=0$  within the whole operating range. Theoretically, this can be achieved by employing a decoupling matrix in the system control. The decoupling matrix must be able to adapt to different operating points and is given for symmetric mains ( $\hat{U}_i=\hat{U}$  and  $\hat{I}_i=\hat{I}$ ) as inverse of the system matrix  $\underline{H}$  (cf. (34)) as

$$\underline{M}_{DEC,SYM} = \underline{H}^{-1}(\hat{U}_i = \hat{U}, \hat{I}_i = \hat{I}) = \frac{2U_0}{(\hat{U} - k_f \hat{I})} \begin{pmatrix} 5\hat{U} - k_f \hat{I} & -(\hat{U} + k_f \hat{I}) & -(\hat{U} + k_f \hat{I}) \\ -(\hat{U} + k_f \hat{I}) & 5\hat{U} - k_f \hat{I} & -(\hat{U} + k_f \hat{I}) \\ -(\hat{U} + k_f \hat{I}) & -(\hat{U} + k_f \hat{I}) & 5\hat{U} - k_f \hat{I} \end{pmatrix}. \quad (35)$$

**Fig.9** shows the realization of the control of the *Y-Rectifier* when employing a decoupling matrix. Generally, also for unbalanced mains the decoupling matrix can be calculated from (33) and (34) but the resulting analytical expressions for the matrix coefficients are very complex what would cause an accordingly high computational effort for adapting the decoupling matrix to the actual operating point.

The output voltage control of each phase module is implemented using a second-order low-pass filter attenuating the DC link voltage ripple with two times the mains frequency (double real pole at  $f=15.9\text{Hz}$ , and/or  $\omega=100\text{s}^{-1}$ ) and a *P*-type controller  $R_{U0}(s)=k_U$ . An integrating part is omitted in order to ensure high system stability also for a remaining low mutual coupling of the phase controls due to inaccuracies of the decoupling matrix. As shown in the following the remaining DC link voltage control error is in the range of 1...2% of the rated DC link voltage which does not pose problems in practice.

According to (35) no decoupling matrix does exist for  $\hat{U}=k_f \hat{I}$  and/or for the operating point where all elements of the system matrix  $\underline{H}$  shows equal values  $H_{ii}=H_{ij}$ . As shown in **Fig.10(a)** for  $k_f=15.2$  the characteristics of  $H_{ii}$  and  $H_{ij}$  intersect within the

operating range at point  $P_S$  indicating a singularity of  $\underline{H}^{-1}$ . By employing an adaptive decoupling matrix  $\underline{M}_{DEC}$  the system could only decoupled for operating points sufficiently differing from  $P_S$ .

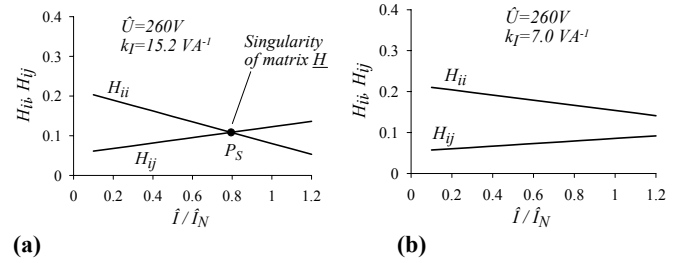


**Fig.10:** Stationary coupling coefficients for  $\hat{U}=0.8 \cdot \hat{U}_n=260\text{V}$  and (a) current controller gain  $k_f=15.2\text{VA}^{-1}$  and (b) current controller gain  $k_f=7.0\text{VA}^{-1}$ .

A solution to this problem is to reduce the current controller gain  $k_f$  in order to achieve  $H_{ii}>H_{ij}$  over the whole operating range. Based on (33)  $H_{ii}>H_{ij}$  can be translated into

$$k_f < \frac{\hat{U}_{min}}{\hat{I}_{max}} \quad (36)$$

where  $\hat{U}_{min}$  denotes the minimum phase voltage amplitude  $\hat{U}_{min}$  and  $\hat{I}_{max}$  is the maximum phase current amplitude of the given operating range. A problem of this approach is that in case of wide-range input voltage the current controller gain  $k_f$  is reduced to very low values. Fulfilling condition (36) automatically fulfills  $H_{ii}>0$  as can easily be proven using (33). **Fig.10(a)** shows the stationary coupling coefficients for  $k_f=15.2$  violating condition (36) which results in the case at hand in

$$k_f < \frac{(0.8 \cdot 325)}{1.2 \cdot (3 \cdot 3500) / (\frac{3}{2} \cdot (0.8 \cdot 325))} \text{VA}^{-1} = 8.0 \text{VA}^{-1} \quad (37)$$

Setting  $k_f=7.0$  fulfills condition (36) and/or (37) (cf. **Fig.10(b)**) and is sufficient for realizing a current controller with low remaining control error and acceptable dynamics within the whole operating range.

**Remark:** Increasing  $k_f$  in **Fig.10(a)** would shift  $P_S$  to the very left hand side and result in  $H_{ii}<H_{ij}$  over a wide operating range. However, close to  $\hat{I}=0$  always  $H_{ii}>H_{ij}$  is remaining so that the singularity in general can only be shifted to small power levels but not completely out of the operating range. Furthermore, increasing  $k_f$  does result in low current control phase margin and therefore is of no further practical interest.

According to **Fig.10(b)**  $k_f=7.0$  results in a pronounced direct coupling  $H_{ii}$  and a comparably weak cross coupling  $H_{ij}$  of the modules. Therefore, a decoupling could be omitted in a first step.

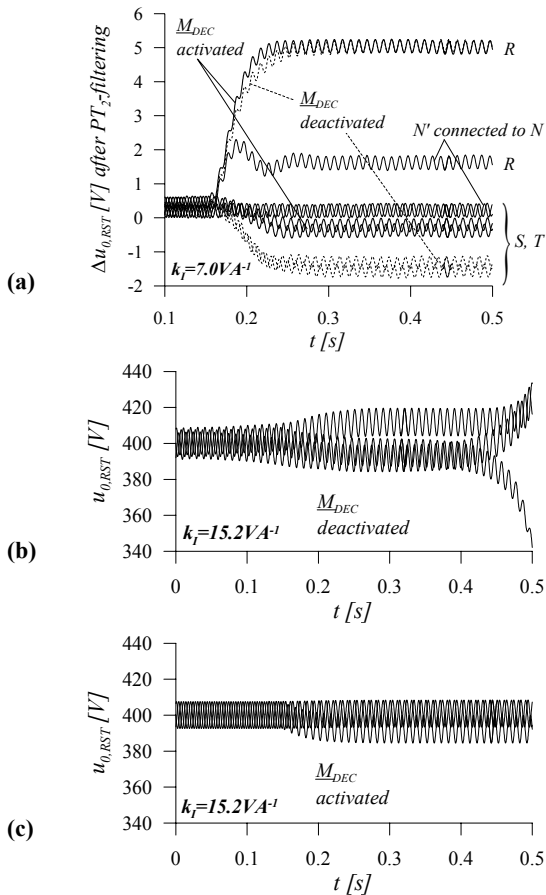


**Fig.11:** (a) Time-behavior of the DC link voltage control errors  $\Delta u_{0,RST}$  of the phase modules (the actual DC link voltages  $u_{0,RST}$  are filtered by a low-pass filter showing a double real pole at  $f=15.9\text{Hz}$ ) in case a step-change of the load ( $\Delta P_{out} = -5\%$ ) of module  $R$  is applied at  $t=0.15\text{s}$ ; the current controller gain is set to  $k_I=7.0$ ; system behavior show for activated and deactivated decoupling matrix  $\underline{M}_{DEC}$  and for connecting the star point  $N'$  to the mains neutral  $N$  (cf. Fig. 1(a)); DC link voltage controller gain set to  $k_{Uf} = 0.00275\text{AV}^{-2}$  except for the case of employing the decoupling matrix where  $k_{Uf} = 0.000275\text{AV}^{-2}$  in order to compensate for the gain introduced by the decoupling matrix. (b) DC link voltages  $u_{0,RST}$  for  $k_I=15.2$  with deactivated decoupling matrix resulting in system instability. (c) Applying  $\underline{M}_{DEC}$  results in stable system operation also for  $k_I=15.2$ . Operating point is  $(80\%U_n@100\%P_n)$  for all simulations.

The most critical operating point then is represented by the combination of  $\hat{U}_{min}$  and  $\hat{I}_{max}$  as  $H_{ij}$  then shows the highest value compared to  $H_{ii}$ . A digital simulation of the system behavior given in this case  $(80\%U_n@100\%P_n)$  is depicted in Fig.11 where the output power of phase module  $R$  is reduced by 5% in a step like manner. Neglecting the coupling (by deactivating the decoupling matrix  $\underline{M}_{DEC}$  in Fig.9) results in stable system operation but causes also deviations of the DC link voltages of the modules of phases  $S$  and  $T$ . These deviations can be significantly reduced by employing an adaptive decoupling according to (35) (cf. Fig.11(a)). Furthermore, in Fig.11(a) a simulation result is shown for the case of connecting the star point  $N'$  to the mains star point  $N$  what results in an ideal decoupling of the three-phase/three-wire system into individual phase modules. The difference in the time-behavior for this ideal hardware-oriented decoupling and the results for applying the adaptive decoupling matrix can be explained by the simplifying assumptions when deriving the system model. The remaining output voltage control error is about 1% of the rated DC

link voltage  $U_n=400$  and therefore does not pose any problem in practice.

In Fig.11(b) the current controller gain is set to  $k_I=15.2\text{VA}^{-1}$  what results in a pronounced cross coupling finally leading to unstable system behavior. Applying a decoupling matrix according to (35) stabilizes system (cf. Fig.11(c)). However, as  $k_I=15.2\text{VA}^{-1}$  is not in accordance with (36) the decoupling could only be maintained for output power levels sufficiently higher or lower than the power level corresponding to  $P_S$  in Fig.10(a). Therefore, this case only demonstrates the correctness of the decoupling but is of no further practical value.

The simulations in Fig.11 are for a load step of 5% which will not occur in practice and, only is used for showing the range of validity of the control theory presented in this paper. For a practical system an unbalance of the modules will mainly be caused by differences in efficiency and therefore will be limited to values well below 1%.

#### IV. CONCLUSIONS

The *Y-Rectifier* combines single-phase unity power factor rectifier modules with isolated DC/DC converter output stages in a three-phase star connection with floating star point  $N'$  and therefore represents an interesting concept for the realization of high power telecommunications power supply systems. However, the missing connection of  $N'$  to the mains neutral  $N$  (cf. Fig.1) results in a cross coupling of the DC link voltage control loops of the phases which is analyzed in this paper. An analytical model is derived which reveals the dependency of the cross coupling term of the system matrix  $\underline{H}$  on the operating parameters and the mains current controller gain. Based on this, an adaptive decoupling could be performed or the current controller gain could be selected such that the cross coupling does not take influence on the system stability.

Future research will focus on the system control for heavily unbalanced mains which will be based on the generally valid analytical expression of the coupling matrix  $\underline{H}$  derived in this paper. Furthermore, the theoretical considerations will be verified for a 10kW *Y-Rectifier* prototype being currently under construction where also the output-oriented DC link voltage control (cf. Fig.1(b)) will be implemented and compared to the input-oriented scheme concerning control performance and realization effort.

#### REFERENCES

- [1] Greul, R., Drofenik, U., Kolar, J.W.: *Analysis and Comparative Evaluation of a Three-Phase Three-Level Unity Power Factor Y-Rectifier*. Proceedings of the 25<sup>th</sup> IEEE International Telecommunications Energy Conference, Yokohama, Japan, Oct. 19 - 23, pp. 421 - 428 (2003).
- [2] Chapman, D., James, D., and Tuck, C.J.: *A High Density 48V 200A Rectifier with Power Factor Correction - An Engineering Overview*. Proceedings of the 15<sup>th</sup> IEEE International Telecommunications Energy Conference, Paris, Sept. 27-30, pp. 118-125 (1993).
- [3] Stögerer, F., Miniböck, J., and Kolar, J.W.: *A Novel Concept for Mains Voltage Proportional Input Current Shaping of a VIENNA Rectifier Eliminating Controller Multipliers. Part II - Operation for Heavily Unbalanced Mains Phase Voltages and in Wide Input Voltage Range*. Proceedings of the 16<sup>th</sup> IEEE Applied Power Electronics Conference, Anaheim (California), USA, March 4 - 8, Vol. 1, pp. 587 - 591 (2001).
- [4] Kolar, J.W.: *Vorrichtung zur Regelung der Zwischenkreisspannungen der Phasenmodule einer Sternschaltung einphasiger Pulsgleichrichter-systeme*. Swiss Patent Application, filed April 2004.